Proceeding of the ASME
2014 International Mechanical Engineering Congress & Exposition
November 14-20, 2014, Montreal, Quebec, Canada

**IMECE2014-38928**

# THERMOFLUID ANALYSIS OF MAGNETOCALORIC REFRIGERATION

**Ayyoub Mehdizadeh Momen**
R&D Staff, Building Equipment Research
Oak Ridge National Laboratory
Oak Ridge, TN, USA
Email: momena@ornl.gov

**Omar Abdelaziz**
R&D Staff, Building Equipment Research
Oak Ridge National Laboratory
Oak Ridge, TN, USA

**Kyle Gluesenkamp**
R&D Staff, Building Equipment Research
Oak Ridge National Laboratory
Oak Ridge, TN, USA

**Edward Vineyard**
Affiliation
R&D Staff, Building Equipment Research
Oak Ridge National Laboratory
Oak Ridge, TN, USA

**Michael Benedict**
Research Engineer
General Electric
GE applience park, Hurstbourne Pkwy, Louisville, KY, 40222

## Abstract

While there have been extensive studies on thermofluid characteristics of different magnetocaloric refrigeration systems, a conclusive optimization study using non-dimensional parameters which can be applied to a generic system has not been reported yet. In this study, a numerical model has been developed for optimization of active magnetic refrigerator (AMR). This model is computationally efficient and robust, making it appropriate for running the thousands of simulations required for parametric study and optimization. The governing equations have been non-dimensionalized and numerically solved using finite difference method. A parametric study on a wide range of non-dimensional numbers has been performed. While the goal of AMR systems is to improve the performance of competitive parameters including COP, cooling capacity and temperature span, new parameters called "AMR performance index-1" have been introduced in order to perform multi objective optimization and simultaneously exploit all these parameters. The multi-objective optimization is carried out for a wide range of the non-dimensional parameters. The results of this study will provide general guidelines for designing high performance AMR systems.

***Keywords:*** Magnetocaloric refrigeration, Non-dimensional analysis, Active magnetic regeneration.

## I. Introduction

Room temperature magnetocaloric refrigeration technology has been extensively studied in recent years as an alternative to the conventional vapor compression refrigeration system. The theoretical performance limit of AMR cooling systems can be substantially higher than conventional vapor compression or absorption systems, however, many challenges including development of low cost magnetic arrays, materials with large magnetocaloric effects, complications with the hydraulic system, heat transfer and material stability hinder its commercial development [1], [2]. Recently, General Electric's (GE) research teams in collaboration with Oak Ridge National Laboratory (ORNL) have announced their intention to commercialize this technology within five years. In order to realize this timeline it will be important to fully investigate the design space including many thousands of possible parameter combinations [3]. In order to understand the details of an AMR and designing a high performance system, many researchers performed numerical studies including model validations. A review of these efforts has been described by Nielsen *et al.* [4]. Most of the previous numerical studies utilize dimensional equations thus the results of these models are only applicable to a very specific system within a narrow range of operating conditions. In this

study however the governing equations were carefully non-dimensionalized and a parametric study using multi-objective optimization has been performed. This study provides generic guidelines for designing the high performance AMR cooling systems.

## II. Governing Equations:

The heat transfer through the generators can be described by taking averages over an elemental volume for both the solid and liquid phase [5]. If radial and azimuthal heat transfer rates are negligible, the energy equation can be assumed as one-dimensional, described as:

$$(1-\varphi)(\rho c)_s \frac{\partial T_s}{\partial t} = (1-\varphi)k_s \frac{\partial^2 T_s}{\partial x^2} - hA_{fs}(T_s - T_f) + (1-\varphi)\dot{q}_s''' \quad (1)$$

$$\varphi(\rho c)_f \frac{\partial T_f}{\partial t} + (\rho c)_f u \frac{\partial T_f}{\partial x} = \varphi k_f \frac{\partial^2 T_f}{\partial x^2} + hA_{fs}(T_s - T_f) + \varphi\dot{q}_f''' \quad (2)$$

where the subscripts *s* and *f* are representative of the solid and fluid phases, respectively. In the above equations $\varphi$ is the porosity, *c* is the specific heat at constant pressure, *k* is the thermal conductivity, $A_{fs}$ is the solid-fluid contact area and $\dot{q}'''$ ($W/m^3$) is the heat produced per unit volume. These two equations are coupled by the convective heat transfer coefficient, *h*:

$$h = \frac{Nuk_f}{D_h}, \quad (3)$$

While the above coupled equations have been frequently used in the literature [4], [6], [7] the presence of the many geometrical heat transfer and fluid flow parameters (16 independent variables) limits the investigation to a predetermined incomplete envelope of operating conditions.

### *Local Thermal Equilibrium Approximation:*

For many magnetocaloric systems local thermal equilibrium is achieved. This occurs when interstitial convective heat transfer coefficient is large and the thermal penetration depth, for a time scale of half the field reversal period, is much greater than the characteristic magnetocaloric material size. For Gadolinium, the thermal penetration depth in one second (corresponding to field frequency of 0.5 Hz) is approximately about 4.6 mm. This implies that for many devices made out of small Gadolinium particles, pellets or thin Gd plates (where thicknesses are generally <<4.6 mm), the local thermal equilibrium may be achieved ($T_s = T_f = T$). This allows further simplification by adding the above equations to obtain a single phase simplified heat equation as follow [5], [8], [9]

$$(\rho c)_m \frac{\partial T}{\partial t} + (\rho c)_f u \frac{\partial T}{\partial x} = k_m \frac{\partial^2 T}{\partial x^2} + \dot{q}_m''' \quad (4)$$

Where subscript *m* refers to volume-averaged mean of phases, and where

$$(\rho c)_m = (1-\varphi)(\rho c)_s + \varphi(\rho c_p)_f \quad (5)$$

$$k_m = (1-\varphi)k_s + \varphi k_f \quad (6)$$

$$\dot{q}_m''' = (1-\varphi)\dot{q}_s''' + \varphi\dot{q}_f''' \quad (7)$$

are, respectively, the volume averaged heat capacity, thermal conductivity, and heat generation per unit volume. While the application of Equation (4) is limited to systems where the heat transfer is near perfect, it provides a very useful single equation with only 8 variables (compared to the original 16 variable) by which a comprehensive parametric study can be efficiently done [8], [9]. A correction for imperfect convective heat transfer (different local fluid and solid temperature) can be implemented simply as heat leak in the generation term with no impact on AMR differential equation [10], [11]. The magnetocaloric property of the material can be estimated by instantaneous temperature change [4], [12] after applying or removing the magnetic field. The magnitude of the temperature change can be estimated from experimental data.

## III. NON-DIMENSIONALIZATION:

The above PDE is non-dimensionalized by selecting appropriate scaling parameters. The dimensionless variables (dimensionless length along generator, elapsed time, fluid velocity, temperature span, and cooling capacity, respectively) are defined as

$$x^+ = \frac{x}{L},\ t^+ = \frac{\mathrm{t}}{\tau},\ u^+ = \frac{u\tau}{L}, T^+ = \frac{T - T_i}{\Delta T_{adi-c}},\ q^+ = \frac{\dot{q}_m''' \forall}{\dot{q}_{cooling}} \quad (8)$$

Where L, $\forall$ , $\tau$ , *u* are the length, apparent volume, hot/cold blows durations (=1/(2*f*); *f* is the system frequency in HZ) and fluid superficial velocity, respectively. Also *T*, $T_i$, $\Delta T_{adi\_c}$ and $\dot{q}_{cooling}$ are the local generator temperature, initial temperature, adiabatic temperature change of material under the applied magnetic field at the Curie temperature and cooling load on the system, respectively. Because of the fairly linear relation between adiabatic temperature change and strength of magnetic field (see Eq. 12) and the definition of non-dimensional temperature span shown in Eq. 8, the non-dimensional simulation results will be approximately independent to the strength of magnetic field. This will help

the model to be very generic. The cooling load can be calculated as

$$\dot{q}_{cooling} = u\varphi A_c (\rho c)_f (T_{amb} - T_{cold\_bath}) \quad (9)$$

where $A_c$ is the cross sectional area of the generator, $\varphi$ porosity and $T_{amb}$ and $T_{cold\_bath}$ are ambient and cold bath temperatures, respectively. Using these dimensionless parameters the following dimensionless version of Equation (4) can be obtained:

$$\frac{\partial T^+}{\partial t^+} + \Phi \frac{\partial T^+}{\partial x^+} = \lambda_1 \frac{\partial^2 T^+}{\partial x^{+2}} + \lambda_2 q^+ \quad (10)$$

where the dimensionless parameters in the above equation are defined as

$$\Phi = \frac{(\rho c)_f}{(\rho c)_m} u^+,\ \lambda_1 = \left(\frac{k_m \tau}{L^2 (\rho c)_m}\right), \text{and } \lambda_2 = \left(\frac{\Phi \varepsilon (T_{amb} - T_{cold\_bath})}{\Delta T_{adi-c}}\right). \quad (11)$$

where $\Phi$ is analogically very similar to the thermal utilization factor (defined as $\dot{m}_f c_f \tau / m_s c_s$ [4]) if the denominator is replaced with solid properties instead of the mixture properties, $\lambda_1$ is representative of the magnitude of the axial thermal diffusion penetration depth in one half cycle verses the length of the generator and $\lambda_2$ represents the magnitude of the cooling load verses the magnetocaloric cooling potential.

## IV. NUMERICAL MODELING

The magnetocaloric effect has been simply considered here as a step change to the temperature at the beginning of the hot and cold blows. In this method, for each control volume, the adiabatic temperature change to the solid, at the corresponding temperature, during the magnetization (or demagnetization) process will be added (or subtracted) to the control volume[4,12]. Nielsen et al. [16] showed a discrepancy between the prediction of the Molecular Field Theory (MFT) and experimental data. Thus in this study, the magnitude of the adiabatic temperature change of material is estimated using a curve fit to the experimental data. This is shown in Fig. 1. The introduced interpolation function provides a superior accuracy for the present simulation and reduces the computational time by 30% compared to conventional interpolation strategies. Note that the computational efficiency is important for the optimization study where thousands of simulations are required in order to obtain conclusive results. The following expressions provide a curve fit with RMSE of 0.04 Kelvin on the adiabatic temperature change of Gd for external magnetic fields below 3 Tesla and temperatures from 250 K to 350 K.

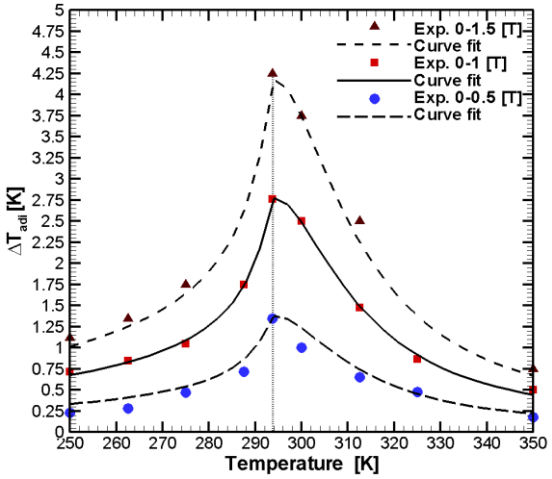


**Fig. 1:** Comparison between Gadolinium adiabatic temperature change [19], [20] with curve fit introduced in Eq. 12.

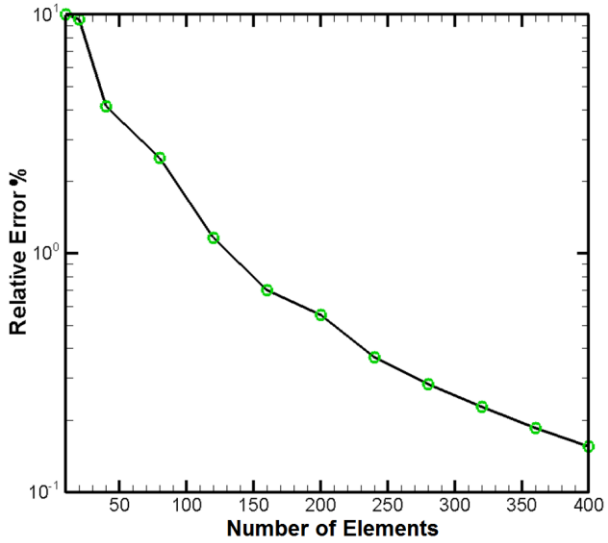


**Fig. 2:** Relative numerical error of the modeling with respect to the number of elements along the regenerator.

$$\Delta T_{adi,Gd}(B,T) = B^{1.009}(a + b \times e^{cT} + d \times e^{fT^2} + g \times e^{hT^3}) \quad (12)$$

, $R^2$=0.99 and B<3 (T)

| | *a* | *b* | *c* | *d* | *f* | *g* | *h* |
|---|---|---|---|---|---|---|---|
| $T<T_{C,Gd}$ | $-5.01316\times10^{3}$ | $5.0124\times10^{3}$ | 0.000001 | $1.9573\times10^{-4}$ | 0.0001 | $1.0817\times10^{-10}$ | 0.0000009 |
| $T>T_{C,Gd}$ | $-4.3859\times10^{3}$ | $4.3878\times10^{3}$ | -0.000001 | $1.7073\times10^{4}$ | -0.0001 | $-7.22773\times10^{9}$ | -0.0000009 |

Equation 10 has been numerically solved using explicit finite difference upwind scheme. The mesh study reveals that the results are mesh independent (relative error <0.1%) for number of elements greater than 360, as shown in Fig. 2. The time step size is also selected so that the maximum relative error in calculation of the temperature at the end of each cycle is less than 0.01%. It was found that the Courant number ($u$·dt/dx) smaller than 0.04 provides relative error less than 0.01%. Therefore, in the following simulations, the number of elements and the Courant number are selected to be 400 and 0.04, respectively.

*Validation of the Model:*

The present numerical modeling has been validated with experimental data of Clot et al [17]. Figure 3 shows that the numerical modeling can well predict the time evolution of the temperature at hot and cold sources especially in the first few cycles. As temperature difference between the cold and hot sources increases Clot *et al.* reported an increase in the thermal losses from their system, resulting in a minor deviation between this ideal model and the experimental data [17].

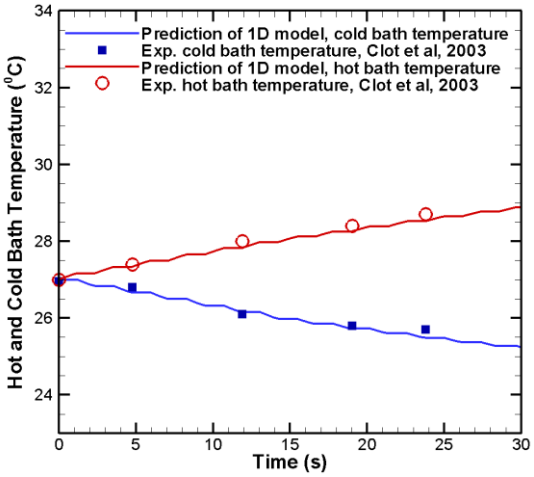


**Fig. 3:** Model validation with the experimental data of Clot et al. [17].

Theoretically, the cooling power and the COP of magnetocaloric refrigerators decrease as the temperature span between cold and hot sources increases. Since Carnot COP is the theoretical limit, it is the most relevant scaling factor for comparing different cooling systems. Therefore, the dimensionless COP often called "refrigerating efficiency" is defined as [18]:

$$COP^{+} = \frac{COP}{COP_{Carnot}} \qquad (13)$$

## V. PARAMETRIC STUDY

There are three important competitive performance metrics for AMR systems; temperature span, cooling capacity and COP. Maximizing one of these metrics might lead to a substantial penalty on the other two. Therefore, a multi-objective optimization needs to be performed in order to find the best tradeoff between these three objectives. There does not exist a single best solution for multi-objective optimizations; instead a number of Pareto optimal solutions may exist. The goal may be to find a representative set of Pareto optimal solutions, and/or quantify the tradeoff in satisfying the different objectives, and/or finding a single solution that satisfies the subjective preferences of a human decision maker (DM). In order to make the parametric study simple, in the next sections we reduce the multi-objective nature of the problem to a single-objective formulation by assuming a uniform weighting to the importance of these dimensionless metrics. A more sophisticated study can be performed by considering DM or market requirements (not considered here).

### *Maximizing Both Temperature Span and Cooling Capacity*

As described earlier, the cooling power of magnetocaloric refrigerators decreases as the temperature span between cold and hot baths increases. Most of the previous studies tried to either maximize the cooling power or maximize the temperature span, however, a reliable cooling system requires both high temperature span as well as high cooling power where both of these conditions cannot be achieved at the same time. Assuming a uniform weighting to the importance of these metrics, in this study we introduce a performance index-1, $\eta_1$," parameter as

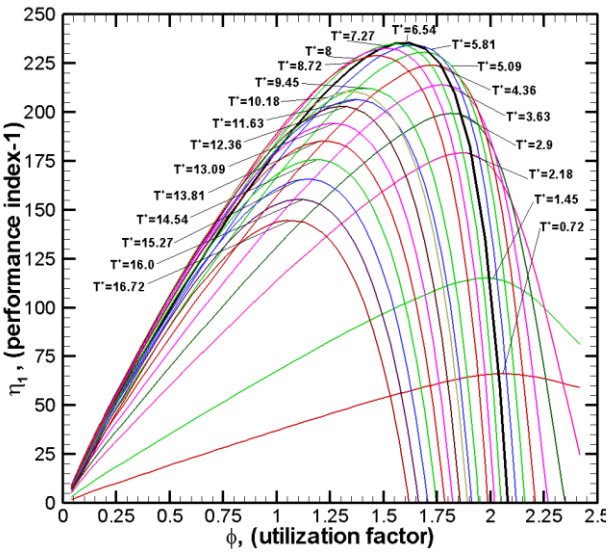


**Fig. 4:** Variation of magnetocaloric refrigeration performance index-1 vs. utilization factor for different non-dimensional temperature spans.

$$\eta_1 = T^{+}.\dot{q}_{cooling} \qquad (14)$$

If the performance index-1 parameter is maximized, this will introduce the operating condition at which both cooling power and the temperature span are relatively high. Note that at the maximum point, where the product is highest, neither temperature span nor the cooling power is at its peak.

More than 3500 cases for a wide range of utilization factor and temperature span have been performed and the conclusive results obtained from these analyses are shown in Figs. 4-5. The temperature span in these simulations varied between $0.72 < T^{+} < 16.72$ (equivalent to dimensional temperature span of $2 < \Delta T < 46^{\circ}C$ across the midpoint of $20^{\circ}C$).

Figure 4 clearly shows that for any specific temperature span, there is a utilization factor at which the $\eta_1$ has a peak. As the temperature span increases this peak shifts toward smaller utilization factors. Interestingly, for Gd material, the ultimate peak of $\eta_1$ takes place at $T^{+}=6.54$ (equivalent to $\Delta T = 18\ ^{\circ}C$) and utilization factor of 1.6. This means that, considering

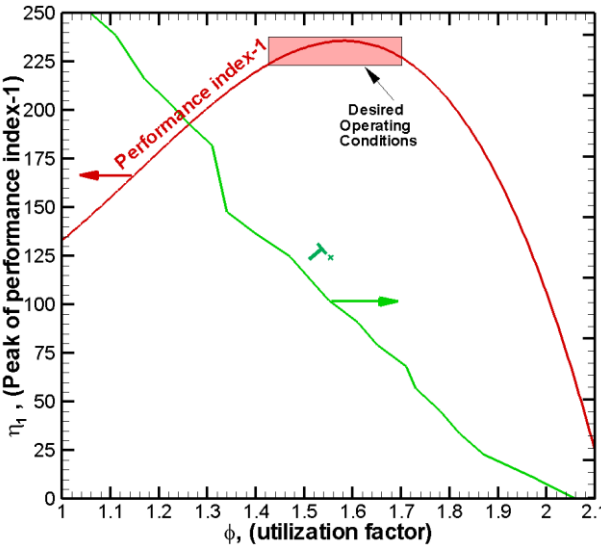


**Fig. 5:** The best operating condition and the associated utilization factor and the performance index at different temperature spans.

cooling capacity and the temperature span, any deviation from this ultimate peak point will lead to a relative penalty either on temperature span or cooling capacity. Such analysis can be generalized to different MC materials or layered stacks of MC materials in order to find the ultimate best operating condition of such a system.

Figure 5 simplifies the representation of this finding and shows that as temperature span increases, a lower utilization is required to get the highest system $\eta_1$. This figure also shows the sensitivity of AMR system to the small deviation from the design condition. For example, this analysis suggests that in the ideal condition, for Gd, the overall system's $\eta_1$ of a magnetocaloric refrigerator operating at design condition of $T^{+}=6.54$ (equivalent to $\Delta T = 18\ ^{\circ}C$) and utilization factor of 1.6, is about 40% superior to that in the same system at temperature span of $T^{+}=16$ (equivalent to $\Delta T = 44\ ^{\circ}C$). Therefore, this analysis suggests useful performance boundaries for Gd operating at different operating conditions.

## VI. CONCLUSION

In this paper a conclusive parametric study has been performed for a wide variety of AMR operating conditions. All governing equations have been non-dimensionalized in order to characterize general behavior of AMR system. Dimensionless analyses help in generalizing the results of this study to be useful for a wide variety of magnetocaloric refrigeration machines. An accurate curve fit of adiabatic temperature changes at different magnetic fields and operating temperatures has been introduced for Gd which significantly reduces computational cost of the model when considering that material. Magnetocaloric performance index-1 has been introduced in order to reduce the multi-objective problem to a single-objective optimization formulation. The results of this optimization show that at each temperature span, there is a unique utilization factor at which the performance index-1 is at the maximum and the ultimate peak of performance index-1 for Gd takes place at dimensionless temperature span of 6.54 and utilization factor of 1.6. This study also quantifies the sensitivity of AMR system performance operating at off-design condition.

## VII. ACKNOWLEDGMENTS

This work was sponsored by the U. S. Department of Energy's Building Technologies Office under Contract No. DE-AC05-00OR22725 with UT-Battelle, LLC.

## VIII. References

[1] J. S. Brown and P. a. Domanski, "Review of Alternative Cooling Technologies," *Applied Thermal Engineering*, vol. 64, no. 1–2, pp. 252–262, Dec. 2013.

[2] A. K. Bingfeng Yu, Min Liu, Peter W. Egolf, "A review of magnetic refrigerator and heat pump prototypes built before the year 2010," *International Journal of Refrigeration*, vol. 33, no. 6, pp. 1029–1060, 2010.

[3] F. J. Michael Benedict, Natarajan Venkat, Edward Vineyard, "GE's Magnetic Refrigeration Breakthrough," Google+Hangout, USA, 2014.

[4] K. K. Nielsen, J. Tusek, K. Engelbrecht, S. Schopfer, a. Kitanovski, C. R. H. Bahl, a. Smith, N. Pryds, and a. Poredos, "Review on numerical modeling of active magnetic regenerators for room temperature applications," *International Journal of Refrigeration*, vol. 34, no. 3, pp. 603–616, May 2011.

[5] D. a. Nield and A. Bejan, "Convection in Porous Media," pp. 31–47, 2013.

[6] J. B. Jensen, K. Engelbrecht, C. R. H. Bahl, N. Pryds, G. F. Nellis, S. a. Klein, and B. Elmegaard, "Modeling of parallel-plate regenerators with non-uniform plate distributions," *International Journal of Heat and Mass Transfer*, vol. 53, no. 23–24, pp. 5065–5072, Nov. 2010.

[7] K. Engelbrecht, "A Numerical Model of an Active Magnetic Regenerator Refrigerator with Experimental Validation," University of Wisconsin-Madison, ISBN 0549634002, 9780549634003, 2008.

[8] A. Rowe, "Thermodynamics of active magnetic regenerators: Part I," *Cryogenics*, vol. 52, no. 2–3, pp. 111–118, Feb. 2012.

[9] A. Rowe, "Thermodynamics of active magnetic regenerators: Part II," *Cryogenics*, vol. 52, no. 2–3, pp. 119–128, Feb. 2012.

[10] S. Schopfer, "experimental and numerical determination of thermohydraulic properties of regenerators subjected to oscillating flow," University of Victoria, 2011.

[11] A. Burdyny, T., Rowe, "Impact of Effective Thermal Conductivity on A Single Phase AMR Model," 2012, pp. 303–308.

[12] A. Tusek, J., Sarlan, A., Zupan, I., Prebil, I., Kitanoviski, A., Poredos, "A numerical optimization of a packed bed AMR," in *Forth International Conference on Magnetic Refrigeration at Room Temperature*, 2010, pp. 425–435.

[13] A. Schopfer, S., Tura, A., Rowe, "Heat transfer and viscous losses in microchannel passive regenerators part II-Parameter extraction," in *Fourth International Conference on Magnetic Refrigeration at Room Temperature*, 2010, pp. 295–304.

[14] S. M. Pineda, G. Diaz, and C. F. M. Coimbra, "Approximation of Transient 1D Conduction in a Finite Domain Using Parametric Fractional Derivatives," *Journal of Heat Transfer*, vol. 133, no. 7, p. 071301, 2011.

[15] G. Strang, "The Heat Equation and Convection-Diffusion," 2006.

[16] K. K. Nielsen, C. R. H. Bahl, a. Smith, R. Bjørk, N. Pryds, and J. Hattel, "Detailed numerical modeling of a linear parallel-plate Active Magnetic Regenerator," *International Journal of Refrigeration*, vol. 32, no. 6, pp. 1478–1486, Sep. 2009.

[17] P. Clot, D. Viallet, F. Allab, a. Kedous-Lebouc, J. M. Fournier, and J. P. Yonnet, "A magnet-based device for active magnetic regenerative refrigeration," *IEEE Transactions on Magnetics*, vol. 39, no. 5, pp. 3349–3351, Sep. 2003.

[18] I.-P. Edition, *ASHRAE Handbook- Fundamentals*. 2013, pp. 2.2–3.

[19] S. Dan'kov, a. Tishin, V. Pecharsky, and K. Gschneidner, "Magnetic phase transitions and the magnetothermal properties of gadolinium," *Physical Review B*, vol. 57, no. 6, pp. 3478–3490, Feb. 1998.

[20] M. Risser, C. Vasile, B. Keith, T. Engel, and C. Muller, "Construction of consistent magnetocaloric materials data for modelling magnetic refrigerators," *International Journal of Refrigeration*, vol. 35, no. 2, pp. 459–467, Mar. 2012.